Modeling of a Magnetocaloric System for Electric Vehicles

A. Noume[*], M. Risser, C. Vasile
LGECO, INSA-Strasbourg
24 Bd de la Victoire, 67084 Strasbourg, France
*E-mail: arsene.nguepnangnoume@insa-strasbourg.fr

Abstract: Magnetic refrigeration system is a promising alternative to traditional refrigeration systems based on gas compression. This technology can be applied in all domains where heat or cold are needed. One of the specific applications of this technology is air conditioning of electric vehicles. This paper presents a model of an Active Magnetic Regenerator (AMR) refrigeration cycle intended for designing a magnetic refrigeration system for an electric vehicle. A two-dimensional model is built and the magnetocaloric effect is modelled. We use for this, interpolating experimental data. The fluid flow is governed by the Navier-Stokes equations and the energy equation governs heat transfer inside solid and fluid. All theses physics are coupled together within the Commercial Software COMSOL Multiphysics. The velocity field, temperature profile, heat transfer coefficient and temperature span of the system are thus determined.

Keywords: Magnetic refrigeration cycle, Air conditioning, Electric vehicle

1. Introduction

Technologies and behaviours in the transport sector must be continuously adapted to new constraints, such as the diminishing supply of fossil energy, climate change, new laws, the increased demand for mobility and safety.
In automotive industry, regardless the type of engine we use, heating and air-conditioning is responsible for the highest energy consumption among all the auxiliary systems all over the year.
For conventional vehicles with thermal engines, the heating of the internal space is easy available because of the heat waste available from the classical engine. The use refrigeration system based on gas compression in an electric vehicle is even more critical than in a thermal motor vehicle. The requirements in heating and the requirements in cooling for an electric vehicle are greater than those of a thermal motor vehicle because, in addition to the needs related to comfort (cooling and heating of the interior),

there are other specific needs, namely cooling of the lithium based battery and power modulator [1], whose temperature must be controlled. The battery, during load and discharge, is prone to increases in temperatures and requires cooling. On starting, when the outside temperature is low it might need to be heated. In addition the power modulator which manages the electricity distribution is also prone to heating and must be cooled. Whereas in a thermal motor vehicle heat is available for free, in an electric vehicle it should be produced with the battery. Because of all these constraints, even by considering the case of heat recovery produced by the battery and the power modulator during their operation, the autonomy of the electric car can be reduced by up to half.

Therefore, using innovative technologies, like magnetocaloric technology for heating and cooling, can improve the performance of standard systems and hereby increase the electric vehicle autonomy.

The magnetic refrigeration technology is based on the so called magnetocaloric effect (MCE) discovered for the first time by Warburg in 1881 [2]. Then Debye [3] and Giauque [4] developed a refrigeration method for very low temperatures, which has been verified experimentally by Giauque and MacDougall in 1933 [5]. Further, new thermodynamic cycles have been developed to reach cryogenic temperature and room temperature.

Experimental results by Zimm et al. [6] published in 1998 show a coefficient of performance (COP) close to 10 with a maximum efficiency of 60 percent of Carnot COP. The power of the system was 600 W and the temperature span was 10K (from 281K to 291K). Since magnetic refrigeration generated a growing interest of industrial, policy makers and researchers. Experimental research as well as theoretical research are oriented today in several domains such as, research on new materials presenting a high level of MCE, research on magnetic field optimisation, research on fluids presenting best thermal properties for heat

transfer, and research on systems behaviour (new cycles, AMR geometry, frequency...).

Recently, a review of numerical modeling of Active Magnetic Regenerators (AMR) around room temperature has been carried out by Nielsen et al. [7].

The applications of this technology are multiple: Industrial processes needing heating or cooling; Transport and Storage of products; Air-conditioning in building, Transport and Aeronautics domains.

This paper presents some aspects of the design of a magnetocaloric system used for the construction of an efficient HVAC unit for electric vehicles.

2. Magnetocaloric HVAC system

Magnetocaloric HVAC system has the advantage that it does not use at all greenhouse gas and others pollutants as classical HVAC does, and it shows higher energy efficiency than the classical gas compression system. Magnetocaloric technology is based on the magnetocaloric effect (MCE) which consists in the variation of the internal energy of magnetic materials, as the result of the magnetic field variation.
Internal energy U of the system can be represented as a function of the entropy S, the volume V and the magnetic field H.

$$U = U(S, V, H) \qquad (1)$$

Correspondingly, the total differential of the internal energy U can have the form:

$$dU = TdS - pdV - MdH \qquad (2)$$

where p is the pressure, T is the absolute temperature, and M represents generalised thermodynamic quantities [8].
Under adiabatic-isobaric process a magnetic field can cause cooling or heating of the material, which is recuperated in order to realise air climate change (cooling or heating) of the space surrounding.
In order to explain the complete cycle of heating and cooling based on MCE, several cycles can be used: Carnot Cycle; Brayton cycle; Ericsson cycle; and the Active Magnetic Regenerator

Refrigeration cycle (AMRR) which is specially adapted to this phenomenon and described here.
The AMRR cycle is made up of four phases:
1) Adiabatic magnetization: the maximum magnetic field is applied and the MCM is warmed up
2) Iso-field heating: heat is absorbed by a coolant blown through the heated MCM, from cold sink to hot sink. Thus, the MCM keeps its initial temperature constant.
3) Adiabatic demagnetization: the magnetic field is decreased to the minimal value, and then MCM temperature decreases.
4) Iso-field cooling: heat is transferred by the coolant blown through the MCM, from hot sink to cold sink.
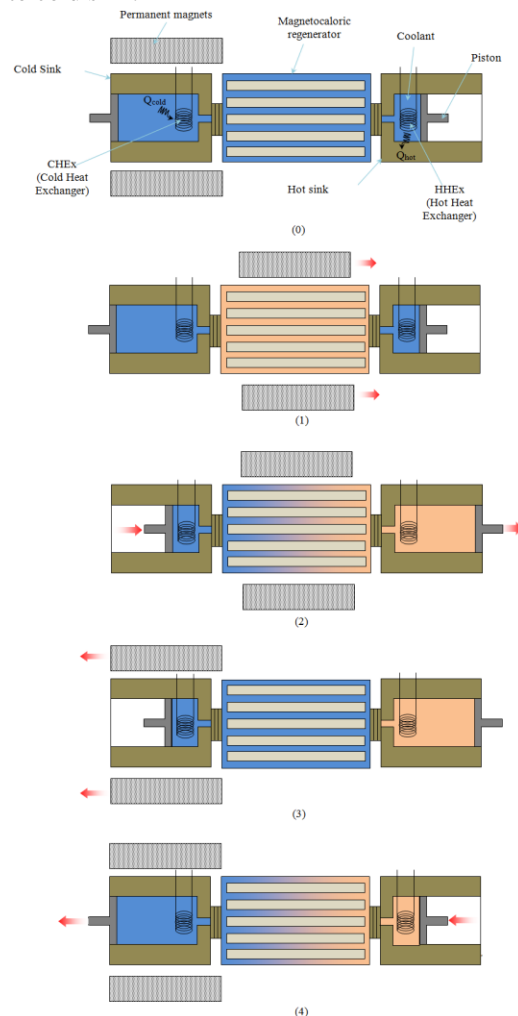
Figure 1. Schematic description active magnetic regeneration refrigeration cycle

The main components of this system are represented in the part (0) of Figure 1, and the parts (1) – (4) describes each one the four phases of the AMRR cycle.

As represented if Figure 1, the magnetocaloric regenerator in our case is composed of several thin parallels plates, alternating with mini-channels containing circulating heat transfer fluid.

The efficiency of the whole system depends directly on the efficiency of the heat transfer between the fluid part and the solid part of the magnetocaloric regenerator, which depends mainly on the value of the convective heat transfer coefficient "h".

Therefore, a numerical simulation of the behaviour of the magnetocaloric regenerator coupled with the circulating fluid is needed. In this way we must study the solutions for optimizing the system efficiency.

In particular, the heat transfer coefficient involved in the heat transfer between MCM and coolant is one of the critical parameters concerned. Then the important study to be carried out is the behaviour of the specific thermodynamic AMRR cycle.

3. Physical model

In our case the physical model is the laminar flow for the fluid and the heat transfer in the fluid and the solid part of the metallic material.

3.1. Mathematical formulation

The complete model is governed by the following equations:

Continuity equation:

$$\nabla \cdot \vec{u} = 0 \qquad (3)$$

Momentum equations:

$$\rho_f (\vec{u} \cdot \nabla) \vec{u} = -\nabla p + \mu_f \nabla^2 \vec{u} \qquad (4)$$

Energy equation:

$$\rho_f C_{p,f} (\vec{u} \cdot \nabla T_f) = k_f \nabla^2 T_f + h\beta (T_s - T_f)_{Int:f/s} \qquad (5)$$

Energy equation governing the heat transfer in the solid:

$$k_s \nabla^2 T_s - h\beta (T_s - T_f)_{Int:f/s} + Q_{MCE} = 0 \qquad (6)$$

The source term Q_{MCE} represents the volumetric heat generation inside the MCM due to the magnetocaloric effect. For a time-dependent model Q_{MCE} is described by the following expression:

$$\dot{Q}_{MCE} = \rho_s C_{P,s} \left(\frac{\partial T_{ad}}{\partial H} \frac{dH}{dt} + \frac{\partial T_{ad}}{\partial T_s} \frac{dT_s}{dt} \right) \qquad (7)$$

At the solid-fluid interface, the following equations are valid:

$$-k_s \frac{\partial T_s}{\partial n} = -k_f \frac{\partial T_f}{\partial n} \qquad (8)$$

$$T_f = T_s \qquad (9)$$

3.2. Boundary conditions

The velocity u of the fluid flowing in contact with the regenerator has a sinusoidal profile, and expressed through equation (10).

$$u(t) = u_0 \sin(2\pi \cdot f \cdot t) \qquad (10)$$

Then we have a changing boundary condition at both ends of the regenerator depending on the sign of u:
When $u(t) > 0$ the inlet temperature of the fluid is $T(x = 0, t) = T_h$.
When $u(t) < 0$ the inlet temperature of fluid is $T(x = L, t) = T_c$.
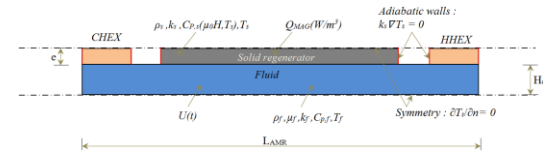At the solid wall the "no slip wall" condition is imposed, then $u = 0$.

Figure 2. Geometrical representation of the model

The Figure 2 represents the geometric configuration of the AMR used in this model.

In this simulation the complete system is working under adiabatic conditions. No thermal energy is exchanged to outside volume. Thus,

values of hot thermal load (q_h) and cold thermal load (q_c) relative successively to hot heat exchanger and cold heat exchanger are zero for this simulation.

The temperature span (ΔT) of the cycle is here given by the difference between the hot end (T_h) temperature measured at HHEx, and the cold end (T_c) temperature measured at CHEx.

These temperature values are directly dependent of the regenerator materials properties and of the efficiency of the heat transfer process. The solid regenerator is made of Gadolinium (Gd), the heat exchangers are made of Copper (Cu), the fluid flowing into the channel is water. The properties of all the materials depending on the temperature parameter are present into the COMSOL library except the properties of Gd which depend on temperature and magnetic field variation (μ_0H).

3.3. Grid Topology

The computational grid represented in Figure 3 is constituted of 27958 free triangular elements and 2 boundary layers with a stretching factor of 1.2.
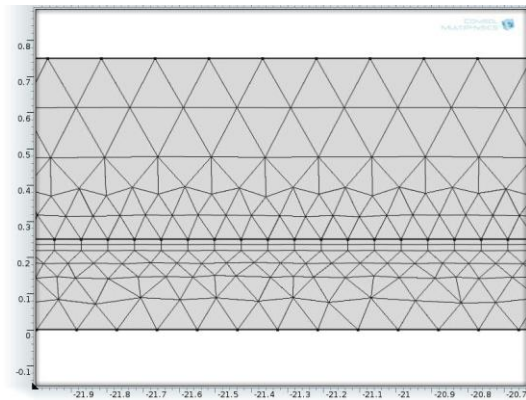

Figure 3. Computational grid of the simulation

4. Use of COMSOL Multiphysics

The complete simulation of the AMR refrigeration cycle takes into consideration more than one physic. In this study laminar flow and heat transfer in a solid and heat transfer in a fluid are the principal physics concerned. COMSOL Multiphysics makes it possible to couple them together in a simple and intuitive way.

The principal difficulty of this simulation is the MCE modeling. The problem is solved by using the interpolation function of COMSOL to interpolate the experimental data of $\Delta T_{ad}(T,\mu_0H)$ and $C_p(T,\mu_0H)$, where both variables are function of two parameters.

The interpolated values of ΔT_{ad} and C_p of gadolinium are represented in the graphics of Figure 4 and Figure 5.
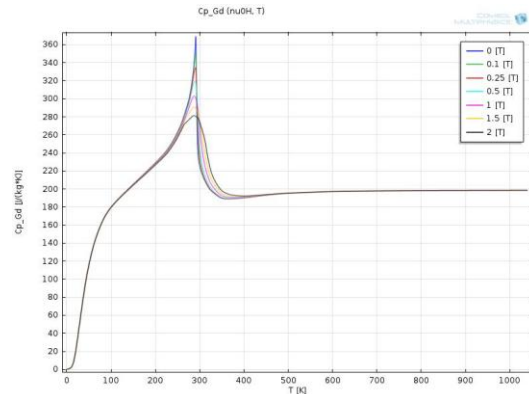

Figure 4. Interpolation of values of specific heat of Gadolinium, Cp (T,μ_0H), using COMSOL

Analysing these figures we must emphasis the important thermodynamic changes for the values of temperature around 300 K which we have called here "room temperature" and under the magnet field variation.
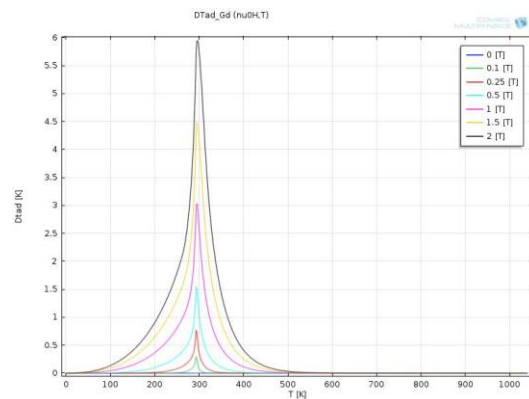

Figure 5. Interpolation of values of adiabatic temperature difference of Gd, $\Delta T_{ad}(T,\mu_0H)$, using COMSOL.

This specific temperature for which significant modifications of ΔT_{ad} and C_p appear under magnetic field variation is called Curie Temperature (T_C). The materials that have this

4

behaviour are called magnetocaloric materials and magnetocaloric alloys respectively.

5. Results and discussion

The model described in the previous sections allows us to analyse the influence of geometrical parameters and fluid parameters on heat transfer coefficient and then on the cycle behaviour.

The knowledge of the velocity profile and velocity values is also important to be known. The velocity field profile is represented in Figure 6. One may observe the classical laminar fluid flow distribution with a maximum value of 0.27 m/s for the velocity in the middle of the channel.

The Navier-Stokes equations are able to model the fluid flow in microchannels. Only one half of the channel is modelled. In our case the height of the channel is $H = 0.2$ mm. The channel width is $W = 50$ mm.
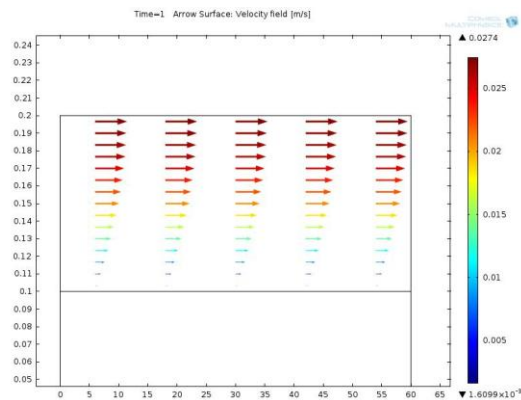

Figure 6. Velocity profile inside the channel

Considering the maximum velocity value shown in Figure 6, and using equations (11) and (12) which express successively Reynolds number and hydraulic diameter, we can determine the Reynolds number.

$$Re = \frac{\rho \cdot v \cdot D_h}{\mu} \tag{11}$$

$$D_h = \frac{2(W \cdot H)}{W + H} \tag{12}$$

Thus the Reynolds number obtained is about 140, for a value of viscosity of water considered at a temperature of the fluid around 300 K. This confirms that the flow is absolutely laminar in our study.

The figure 7 represents the temperature variation all over the system during the hot blow period. The fluid domain (160 mm x 0.5 mm) presents a minimum temperature of 287 K and a maximum temperature of 300 K. The fluid domain is coupled to the solid domain (60 mm x 0.5 mm) which presents a minimum temperature of 287K and a maximum temperature of 297 K.
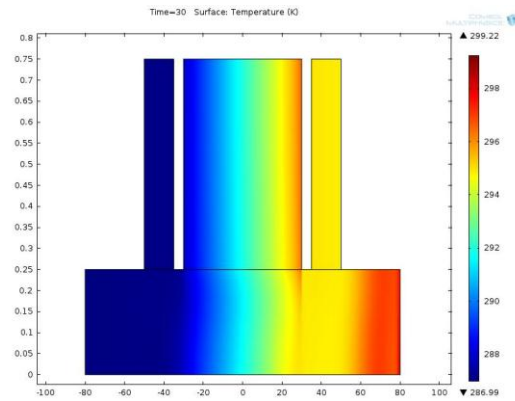
Figure 7. Temperature profile of the system during the hot blow period

The heat transfer coefficient "h" is determined in the postprocessing step through the following equation:

$$h = \frac{q_{wall}}{T_{wall} - T_{fluid,average}} \tag{13}$$
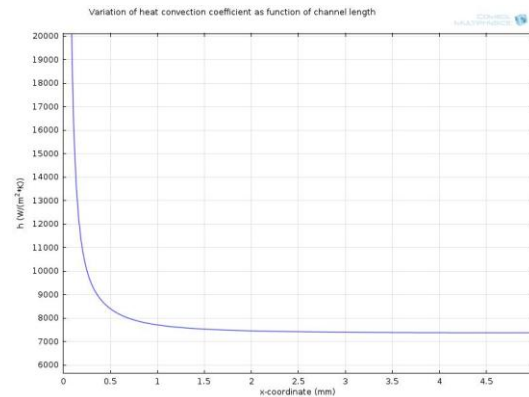
Figure 8. Variation of heat transfer coefficient along the axial coordinate of the channel

The Figure 8 represents the evolution of the heat transfer coefficient variation along the channel length.

The value of heat transfer coefficient 'h' at point $x = 0$, as we can see, is infinite. This is due to the fact that T_{wall} and T_{fluid} at that specific point

5

are equal. Of course, this is unrealistic. Except this, the graphic obtained is a good result of the convective heat transfer coefficient.

The graphic represented in Figure 9 is the result of the AMR refrigeration cycle simulation. The hot end and cold end temperatures variation with time are represented. The difference between the maximum and the minimum temperature value gives us the temperature span of the system. In this case de span temperature is close to 8 K.

The best solution researched is the highest temperature span possible. It is possible to reach a larger temperature span with some new materials and alloys presenting improved thermal properties.

Another way to obtain higher temperature span is to combine in series several material beds, from the bed characterized by the lower Curie temperature to the higher Curie temperature.
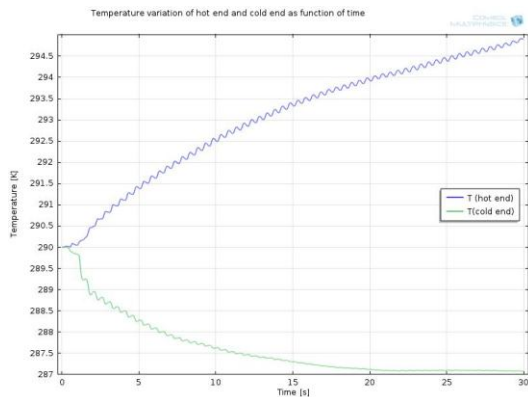
Figure 9. Variation of the hot end and cold end temperature in time

6. Conclusions

The aim of this paper was to study and understand the behaviour of a magnetocaloric system, particularly a room temperature AMR refrigeration cycle. To reach this goal a two-dimensional model is built and analysed. This model allows the assessment of the behaviour of the magnetocaloric HVAC in order to improve its design and its driving parameters.

7. References

1. Michael R. Giuliano, Suresh G. Advani, Ajay K. Prasad. Thermal analysis and management of lithium–titanate batteries, Journal of Power Sources, **196**, 6517–6524 (2011)

2. E. Warburg, Magnetische Untersuchungen über einige Wirkungen der Koerzitivkraft, Ann Phys, **13**, 141–164 (1881)

3. P. Debye, Einige Bemerkungen zur Magnetisierung bei tiefer Temperatur, Ann Phys, **81**, 1154–1160 (1926)

4. W.F. Giauque, A thermodynamic treatment of certain magnetic effects. A proposed method of producing temperatures considerably below 18 absolute, J Am Chem Soc, **49**, 1864–1870 (1927)

5. W.F. Giauque, D.P. MacDougall, Attainment of temperatures below 18 absolute by demagnetization of $Gd_2(SO_4)_3 \cdot 8H_2O$, Phys Rev Lett, **43 (9)**, 768 (1933)

6. C. B. Zimm, A. Jastrab, A. Sternberg, V. Pecharsky, K. Gschneider, M. Osborne, I. Anderson, Description and performance of a near-room temperature magnetic refrigerator, Advances in Cryogenic Engineering, **43**, 1759–1766 (1998)

7. K.K. Nielsen, J. Tusek, K. Engelbrecht, S. Schopfer, A. Kitanovski, C.R.H. Bahl, A. Smith, N. Pryds, A. Poredos, Review on numerical modeling of active magnetic regenerators for room temperature applications, International Journal of Refrigeration, **34**, 603–616 (2011)

8. A.M. Tishin, Y.I. Spichkin, The magneto-caloric effect and its applications, 475, Institute of Physics, Publishing Bristol and Philadelphia London (2003).

8. Acknowledgements

6